New Journal of Physics
The open-access journal for physics

Double-slit experiment with a polyatomic molecule: vibrationally resolved C 1s photoelectron spectra of acetylene

L Argenti[1], T D Thomas[2], E Plésiat[1], X-J Liu[3,4], C Miron[4], T Lischke[3], G Prümper[3], K Sakai[3], T Ouchi[3], R Püttner[5], V Sekushin[5], T Tanaka[6], M Hoshino[6], H Tanaka[6], P Decleva[7], K Ueda[3,9] and F Martín[1,8,9]

[1] Departamento de Química, Módulo 13, Universidad Autónoma de Madrid, 28049 Madrid, Spain
[2] Department of Chemistry, Oregon State University, Corvallis, OR 97331, USA
[3] Institute of Multidisciplinary Research for Advanced Materials, Tohoku University, Sendai 980-8577, Japan
[4] Synchrotron SOLEIL, L'Orme des Merisiers, Saint-Aubin, BP 48, 91192 Gif-sur-Yvette Cedex, France
[5] Institut für Experimentalphysik, Freie Universität Berlin, Arnimallee 14, D-14195 Berlin, Germany
[6] Department of Physics, Sofia University, Chiyoda-ku, Tokyo 102-855, Japan
[7] Dipartimento di Scienze Chimiche, Universitá di Trieste, 34127 Trieste, and CNR-IOM, Trieste, Italy
[8] Instituto Madrileño de Estudios Avanzados en Nanociencia (IMDEA-Nanociencia), Cantoblanco, 28049 Madrid, Spain
E-mail: ueda@tagen.tohoku.ac.jp and fernando.martin@uam.es

New Journal of Physics **14** (2012) 033012 (18pp)
Received 5 December 2011
Published 12 March 2012
Online at http://www.njp.org/
doi:10.1088/1367-2630/14/3/033012

Abstract. We report the first evidence for double-slit interferences in a polyatomic molecule, which we have observed in the experimental carbon 1s photoelectron spectra of acetylene (or ethyne). The spectra have been measured over the photon energy range of 310–930 eV and show prominent oscillations in the intensity ratios $\sigma_g(\upsilon)/\sigma_u(\upsilon)$ for the vibrational quantum numbers $\upsilon = 0, 1$ and for the ratios $\sigma_s(\upsilon = 1)/\sigma_s(\upsilon = 0)$ for the symmetry $s = g, u$. The experimental findings are in very good agreement with *ab initio* density

[9] Authors to whom any correspondence should be addressed.

functional theory (DFT) calculations and are compatible with the Cohen–Fano mechanism of coherent emission from two equivalent atomic centers. This interpretation is supported by the qualitative predictions of a simple model in which the effect of nuclear recoil is taken into account to the lowest order. Our results confirm the delocalized character of the core hole created in the primary photoionization event and demonstrate that intramolecular core-hole coherence can survive the decoherent influence associated with the asymmetric nuclear degrees of freedom which are characteristic of polyatomic molecules.

Contents

1. Introduction

When a homonuclear diatomic molecule is photoionized from a delocalized orbital, the photoelectron amplitudes originating from the vicinity of either one or the other of the two nuclei give rise to interference fringes, which remind us of Young's double-slit experiment. This phenomenon was suggested by Cohen and Fano [1], almost half a century ago, as a tentative explanation of some unexpected 'shoulders' in the inner-shell photoionization cross sections of N_2 and O_2, as a function of the photoelectron energy [2]. As it was originally conceived, the Cohen–Fano model applies to the photoionization of H_2^+, where only the $1s\sigma_g$ molecular orbital is occupied and is approximately written as

$$1s\sigma_g = \frac{1s_a + 1s_b}{\sqrt{2(1+S)}}, \quad S = \langle 1s_a | 1s_b \rangle, \tag{1}$$

where $1s_{a(b)}$ is the 1s orbital centered in nucleus a (b). The dipole photoionization amplitude in plane wave approximation, $\mathcal{A}_{\vec{k}}$, is then proportional to the sum of the photoionization amplitudes associated with the two atomic centers, separated by a distance R, which results in constructive and destructive interference fringes along specific directions with respect to the internuclear axis

$$\mathcal{A}_{\vec{k}} = \langle \vec{k} | \hat{\epsilon} \cdot \vec{p} | 1s\sigma_g \rangle \propto 2(\hat{\epsilon} \cdot \vec{k}) \langle \vec{k} | 1s \rangle \frac{\cos(\vec{k} \cdot \vec{R}/2)}{\sqrt{2(1+S)}} \, e^{-i\vec{k}\cdot\vec{R}_{cm}}, \tag{2}$$

where $\vec{k}$ is the momentum of the ejected electron, $\hat{\epsilon}$ is the polarization direction of the incident light, $\vec{p}$ is the dipole operator, $\vec{R}$ is the internuclear distance vector and $\vec{R}_{cm}$ is the center-of-mass position vector. Signatures of these interferences remain even when averaged over the molecular orientations as oscillations of the total cross-section as a function of the photon energy

$$\sigma = \frac{\sigma_H}{1+S}\left(1 + \frac{\sin kR}{kR}\right), \tag{3}$$

where σ_H is the atomic photoionization cross section. Evidence of such a two-center coherent emission is thus expected in the photoelectron angular distribution in the molecular frame as well as in the total cross section. Experimental demonstration of these effects, however, is challenging due to the rapid decrease of the total cross section with the photoelectron energy together with the relatively high energy that needs to be reached either to highlight interference patterns in the photoelectron angular distribution in the body-fixed frame, or to cover a full oscillation period in the total cross section as a function of the photon energy.

As a consequence, several years passed before direct evidence for double-slit interferences was actually recorded. The first were observed in the ionization of H_2 caused by the collision with positively charged ions [3, 4]. Signatures of this effect were later recognized also in electron-impact ionization of D_2 [5] and of H_2 [6]. In order to disentangle the oscillations from the rapidly decreasing background, the observed cross sections had to be compared with some reference ones where the effect of the expected multi-center interferences is absent. For the interpretation of (e,2e) cross sections [6], for example, H_2 was compared with He, which is the natural realization of the united-atom limit of the hydrogen molecule. In most cases, however, comparison is made with theoretical estimates of somewhat arbitrary atomic cross sections. A quantitative determination of these interferences depends very much on the particular reference used in such comparisons.

An unambiguous determination of double-slit interference was eventually accomplished by studying double ionization of H_2 with synchrotron radiation in association with a COLTRIMS detection [7, 8]. In these latter experiments, the molecule is stripped of both electrons and all the charged fragments are detected in coincidence, thus making it possible to reconstruct the angular distribution of the two electrons in the molecular frame. At extreme unequal energy sharing the fast electron displays interference fringes in agreement with the predictions of a modified Cohen–Fano model that accounts for the interaction of the photoelectron with the two bare nuclear charges [9].

Interference effects arising in the photoionization of molecular hydrogen are now well understood from a theoretical point of view [10–13]. In particular, it has been realized that double-slit interferences are strongly affected by the vibrational motion of the nuclei. This aspect offers the opportunity for solving in an elegant and consistent way the problem of the rapid decrease of the cross section with the energy when, instead of the molecular-frame photoelectron angular distribution, only integral photoelectron cross sections are measured, i.e. by monitoring the ratios between vibrationally resolved photoelectron cross sections, as opposed to the unresolved total cross section itself. This is so because partial cross sections are subject to a comparable decrease with the photon energy, but are unequally affected by the two-center interferences. High-resolution third-generation synchrotron facilities have made it possible to resolve the photoelectron peaks corresponding to different vibrational states of the parent ion, thus demonstrating unambiguously and conclusively the original Cohen–Fano prediction [14].

Cohen–Fano effects are visible whenever photoionization takes place from a well-defined molecular orbital that is significantly delocalized over two nuclei. In polyelectronic homonuclear diatomic molecules, e.g. N_2, this is the case for some valence orbitals. Indeed, clear signatures of Young-type interference effects in the ratio between vibrationally resolved cross sections in the photoionization of N_2 from the valence shell were revealed both experimentally and theoretically [14, 15]. The strongest photoelectron signal at high energy, however, is due to core rather than to valence electrons. For core electrons, the situation is

complicated by the circumstance that both the $1s\sigma_g$ and the $1s\sigma_u$ core orbitals are occupied:

$$1s\sigma_{g/u} = \frac{1s_a \pm 1s_b}{\sqrt{2(1 \pm S)}}. \tag{4}$$

This fact has two consequences. Firstly, the interference fringes from the two molecular orbitals are in phase opposition [16]. As a result, if the corresponding photoelectrons are not disentangled, the interference pattern from one orbital cancels that from the other. Secondly, in contrast with the H_2 case, the core-hole states of polyelectronic molecules are not stable; instead, they relax through Auger decay or x-ray fluorescence. For nitrogen and carbon, for example, the characteristic lifetime is only a few femtoseconds, which corresponds to a natural linewidth of $\sim$100 meV. To uncover double-slit interferences, the energy separation between the σ_g and the σ_u orbitals must be larger than, or at least comparable to, their natural linewidths. This is the case for N_2 [16–20], because the strong triple covalent bond that binds the two atoms brings them close enough to induce a significant superposition between the two core orbitals, which results in an energy splitting between their symmetry-adapted combinations of as much as $\sim$100 meV [21].

Given the wealth of evidence for double-slit interferences in nitrogen [16–20, 22], the question arises as to whether a similar phenomenology can be observed also in systems larger than diatomics. The answer is not obvious, since polyatomic molecules feature several vibrational modes, some of which are not totally symmetric. As a result, degenerate electronic levels may be unstable and split, through vibronic coupling (the Renner–Teller effect in linear molecules [23–27]), by spontaneously breaking the molecular symmetry. For closely energy-spaced core holes, the symmetry break results in a localization of the core hole [28, 29]. The idea that core holes in polyatomic molecules should be regarded as being always localized altogether has been around for quite some time (e.g. [30–32]). For example, data available for C_2H_6 (ethane) and C_2H_4 (ethene) show that the energy separation between the σ_g and the σ_u core holes is too small ($\leqslant$50 meV [33–35]) to be compatible with delocalized core holes.

Acetylene differs significantly from ethane and ethene, because its C–C bond length is smaller, 1.203 Å [36] versus 1.536 and 1.337 Å, respectively, and comparable to that of nitrogen, 1.112 Å. Thus, one could reasonably expect that double-slit interferences associated with delocalized core holes, i.e. large core-hole σ_u/σ_g energy splittings, should also exist for acetylene. However, this splitting [34] is comparable to the frequency of the stretching modes of the molecule and, as a result, the $^2\Sigma_u^+(\upsilon = 1)$ state of the antisymmetric carbon–hydrogen stretching mode is partly mixed with the $^2\Sigma_g^+(\upsilon = 0)$ state [37]. Still, the most prominent signal corresponds to the excitation of the totally symmetric C–C normal mode, which suggests that this is the normal mode that one should ideally choose to observe double-slit interference effects. Nevertheless, the issue of core-hole localization versus delocalization in acetylene is still far from being settled. Indeed, measurements of the σ_u/σ_g ratio reported by Thomas *et al* [38] and Hoshino *et al* [39] have shown no indications of double-slit interferences, likely due to the fact that the photon energy only extended up to 50–60 eV from the threshold. Furthermore, in the context of asymmetric molecular fragmentation, evidence of core-hole localization has been reported [40] and similar considerations have also been expressed by Osipov *et al* [41].

In this paper, we present the first evidence of the Cohen–Fano interferences in vibrationally resolved C1*s* photoionization of acetylene. As the $1\sigma_g$ and $1\sigma_u$ core-hole states are individually resolved, oscillations can be clearly seen both in the ratio of the same vibrational levels in the two electronic channels (e.g. $\upsilon = 0$ in the $1\sigma_u/1\sigma_g$ ratio) and in vibrational branching

ratios $\upsilon = 1/\upsilon = 0$ in each separate electronic channel, $1\sigma_g$ and $1\sigma_u$. Both ratios are free from the rapid decrease of the corresponding cross section with photoelectron energy. These results demonstrate conclusively that, in the case of acetylene, (i) delocalized core holes are created following photoelectron emission, (ii) the interferences are not washed out by decoherence effects induced by the possible vibronic coupling with asymmetric nuclear degrees of freedom and therefore (iii) Cohen–Fano interferences are not restricted to diatomic molecules. The experimental values for the $\sigma_g(\upsilon)/\sigma_u(\upsilon)$ ($\upsilon = 0,\ 1$) ratios compare well with the theoretical predictions of a *first-principles* density functional theory (DFT) calculation, which includes only the C–C symmetric stretching mode and which has already reproduced successfully the vibrationally resolved photoionization cross sections of CO, N_2 [14] and CH_4 molecules [42]. The interpretation of the observed behavior in analogy to double-slit interferences is confirmed by a comparison with the prediction of a simple model, in which recoil effects and intramolecular photoelectron scattering are included at the lowest order. Within this model, it is also apparent that the effect of the photoelectron amplitudes that originate from the scattering on the two hydrogen atoms is negligible. In this respect, acetylene bears a close resemblance to the N_2 molecule.

The paper is organized as follows. In sections 2 and 3, we describe the experimental and theoretical methods used in this work. Then the results are presented and discussed in the framework of a simple model. Conclusions and future prospects are presented in section 5.

2. Experimental methods

Experiments have been carried out at three different facilities: Spring8 (Japan), SOLEIL (France) and ALS (USA). The results of the latter are restricted to low photoelectron energies and have been published elsewhere [38], so they will not be described here.

The details of the SPring-8 experiment are similar to those described elsewhere [16, 43]. Briefly, we used the high-resolution soft x-ray photochemistry beam line 27SU [44] (a figure-8 undulator) which provides linearly polarized radiation, whose polarization axis can be selected either horizontal or vertical by changing just the undulator gap, without changing any other optics. In the present measurements, photoelectrons were detected at zero angle with respect to the polarization vector. The heart of the electron spectroscopy apparatus is a 20 cm radius hemispherical electron energy analyzer (Gammadata-Scienta SES-2002). In the present experiment, the analyzer bandwidth was set to ∼31 meV, whereas the monochromator bandwidth was set to 1/10 000 of the photon energy. The overall bandwidth, i.e. a convolution of the monochromator and analyzer bandwidths, was determined separately by measuring Xe 5p photoelectrons at the same monochromator and analyzer settings.

In the SOLEIL experiment the data have been collected at the soft x-ray PLEIADES beamline for isolated species spectroscopies [45]. This beamline, briefly described in [46–48], benefits from the improved spectral brightness of SOLEIL combined with innovative x-ray optics and instrumentation. An 80 mm period Apple II undulator was used, making it possible to cover the energy range of 35–1000 eV with any kind of polarization starting from 55 eV. The measurements were carried out using a wide-angle lens VG-Scienta R4000 electron spectrometer installed at a fixed position, with the electron detection axis perpendicular to the storage ring plane. X-ray light polarization was set at the magic angle of 54.7° with respect to the electron detection axis. The gas pressure in the spectrometer vacuum chamber was kept constant at about 8×10^{-6} mbar for all measurements.

A 1600 lines mm^{-1} grating has been used with a monochromator slit of 30 μm for most of the measurements, corresponding to a photon bandwidth better than 16 meV at 350 eV. The electron spectrometer has been operated at a 20 eV pass energy at 350 eV excitation energy and 50 eV pass energy for higher excitation energies using a curved slit of 200 μm, providing a theoretical kinetic energy resolution of 10 and 25 meV, respectively. The spectra were additionally broadened by well-known translational and recently discovered rotational Doppler broadening effects [49, 50] due to the thermal motion of gas-phase molecules at room temperature. During the measurements, the storage ring was operated in top-up mode with a constant electron current of 401 ± 1 mA, and the photon intensity was monitored using an AXUV100 silicon photodiode from IRD Inc. Spectra were normalized with respect to gas pressure, photon flux and measurement duration and were energy calibrated with respect to the published value for the C1s photoionization energy in C_2H_2 of 291.179 eV [51].

For the analysis of the spectra we have used a least-squares fitting procedure [52] to fit eight peaks to each spectrum. These correspond to the $v = 0$, 1, 2 and 3 vibrational excitations of the C–C stretching mode, with one series of four peaks for the u states and one series for the g states. Since the $v = 3$ peak has low intensity, its spacing with respect to the $v = 2$ peak is fixed to be the same as the spacing between the $v = 2$ and $v = 1$ peaks. Otherwise the positions and intensities of the peaks are free parameters in the fitting procedure. The peak shapes take into account the Lorentzian lifetime width, an instrumental broadening that is assumed to be Gaussian, and the effect of the interaction between the Auger electron and the photoelectron (post-collision interaction (PCI). For the PCI line shape, we have used equation (8) of van der Straten *et al* [53] at photon energies close to threshold and equation (12) at higher energies. For each set of experiments we have used values for the instrumental resolution that were indicated by the settings of the monochromator and the electron spectrometer. For the SPring-8 data, measurements of the xenon $5p_{3/2}$ photoelectron spectra indicate that the actual resolutions are in agreement with those predicted. The effects of both translational and rotational [49, 50] Doppler broadening have been included in our estimates of the instrumental line width. The Lorentzian width is a fitting parameter, and we have assumed that there is a single value, common to both the u and g states. Other fitting models that we have explored include using six or nine peaks instead of eight, allowing the Lorentzian widths to be different for the u and g states, and allowing the Lorentzian widths to be completely free. These models lead to higher values of χ^2 or to a high degree of correlation between the fitting parameters or to inconsistencies among the various groups of data.

We can expect that some of the free parameters, such as the spacing between the peaks, will be the same in all of the spectra. To take advantage of these expectations, we have fit the data in five groups (three for the SPring-8 data and one each for the ALS and SOLEIL data) with certain parameters constrained to be the same for each spectrum within the group. The photon energy ranges for each group are listed in table 1.

The parameters that have been derived from these fits for the five groups are summarized in table 1. These include the Lorentzian width, Γ_L, the g–u splitting for the $v = 0$ states and the vibrational fundamental frequencies, υ_u and υ_g, for the C–C symmetric stretching mode.

The general agreement of the derived parameters is good. This is a striking result, considering that there are 39 spectra included in the analysis, spanning a wide range of energies, with different contributions from PCI, different contributions from instrumental and Doppler broadening, and different relative intensities of the g and u components. Although this agreement does not prove that the assumptions made for the analysis are valid, a failure to

Table 1. Parameters derived from fits. Values in parentheses are standard deviations of the distribution.

Group	$h\upsilon$ (eV)	Γ_L (meV)	g–u (meV)	υ_u (meV)	υ_g (meV)
SP8-L	296–314	97.7	103.1	264.9	275.9
SP8-M	316–350	98.6	102.8	264.3	277.1
SP8-H	320–934	92.5	103.2	264.0	276.7
ALS	310–340	101.8	102.4	265.0	276.8
SOLEIL	350–500	107.8	102.0	265.0	278.2
Average		100.0(6)	102.7(0.5)	264.6(0.5)	276.9(0.8)

find consistency among the results obtained from the different groups would certainly call into question these assumptions.

The average value of the Lorentzian linewidth, 100 meV, is consistent with linewidths that have been found for carbon 1s photoelectron spectra in other compounds [54]. The average value of the g–u splitting, of 102.7 meV, is close to the value of 101.6 ± 0.8 meV given by Börve *et al* [37]. The two values of the C–C stretching frequency are slightly higher than those reported by Börve *et al*, but agree with their result that the frequency for g vibration is slightly higher than that for the u vibration.

3. Theoretical methods

The vibrationally resolved photoionization cross section is evaluated to first order of perturbation theory within the Born–Oppenheimer and dipole approximations:

$$\sigma_\alpha\left(v, v', \omega\right) = \frac{4\pi^2\omega}{3\hbar c} a_0^2 \sum_\eta \sum_{l_\eta} \left|T_{\alpha_\eta l_\eta v v'}\left(\varepsilon\right)\right|^2, \tag{5}$$

where

$$T_{\alpha_\eta l_\eta v v'}\left(\varepsilon\right) = \int \chi^*_{M,v}\left(R\right) \mu_{\alpha_\eta l_\eta}\left(\varepsilon, R\right) \chi_{M^+_\alpha, v'}\left(R\right) \mathrm{d}R, \tag{6}$$

$\mu_{\alpha_\eta l_\eta}$ is the dipole–transition matrix element between the initial electronic state, ψ_0, and the final electronic continuum state, $\psi_{\alpha_\eta l_\eta}$, of C_2H_2, α denotes the electronic state of the residual ion, η is the symmetry of the final state, $\chi_{M,v}$ is the initial vibrational state, $\chi_{M^+_\alpha, v'}$ is the final vibrational state, ω is the photon energy and ε is the photoelectron energy.

To evaluate the electronic continuum state $\psi_{\alpha_\eta l_\eta}$, we have used an extension of DFT, originally developed by Decleva and coworkers to treat molecular ionization at the molecule's equilibrium position (see [55] and references therein). The method has been shown to provide accurate photoionization cross sections for simple as well as for very complex molecules (see, e.g., [55]). Here the method has been extended to describe non-equilibrium geometries. In particular, we have considered 71 different geometries associated with the C–C symmetric stretching mode. They have been built by symmetrically varying the C–C distance while keeping the C–H distance at its equilibrium value. A standard local density approximation (LDA) functional has been used to describe exchange and correlation effects.

For each value of the C–C distance, we have followed the following procedure. The initial Kohn–Sham orbitals have been generated by running a standard preliminary LCAO-DFT calculation (LCAO stands for linear combination of atomic orbitals) with the program Amsterdam Density Functional (ADF) (see [56] and references therein) using an LDA functional in a double zeta-polarization (DZP) basis set. The resulting ground state density is then used to build the Hamiltonian matrix in a new basis set of B-spline functions B and real spherical harmonics Y^R:

$$\xi^i_{\alpha l_\alpha j}(r,\theta,\phi) = \sum_{k=1}^{N^i_{\rm eq}} \frac{1}{r_k} B_j(r_k) \sum_{m_\alpha=-l_\alpha}^{l_\alpha} b_{\alpha l_\alpha m} Y^R_{l_\alpha m}(\theta_k,\phi_k), \tag{7}$$

where α gathers the indexes referring to a specific irreducible representation (IR), l_α and m_α correspond to the usual angular momentum quantum numbers, i and k indicate, respectively, the ith non-equivalent expansion center and its kth equivalent subspecies, $N^i_{\rm eq}$ denotes the number of equivalent centers associated with i, the index j refers to the jth B-spline, r, θ and ϕ stand for the spherical coordinates in the molecular framework and $b_{\alpha l_\alpha m}$ are the coefficients of the symmetry adapted linear combination of real spherical harmonics. The non-equivalent centers can be divided into two categories:

- The one-center expansion (OCE) that is unique (as its name implies) and located at a chosen origin. Its radius is large (40 au in the present calculation), which allows us to properly treat the long-range oscillatory behavior of the continuum wavefunction.
- The off-center expansions located at the center of each non-equivalent nucleus in order to describe more accurately the sharpness of the bound-state wavefunctions. The expansion-interval is cut off and is generally quite small (0.5 au in the present calculation) in order to avoid linear dependencies due to excessive overlap with other basis functions. It has been observed that the introduction of the off-centers into the OCE B-spline improves dramatically the convergence of the calculation for most molecules.

In the particular case of acetylene, the OCE is centered in the symmetry center of the molecule and only two off-center expansions are required to take care of the carbon and hydrogen atoms. Hence, the radial part of the basis functions is defined by three sets of $N_{\rm b}$ one-dimensional B-spline functions, built on two different radial intervals: $[0; R^0_{\rm max}]$ for the OCE set $\{\xi^0_{\alpha l_\alpha}\}$ and $[0; R^i_{\rm max}]$ for the off-centers set $\{\xi^i_{\alpha l_\alpha}\}$. The LCAO basis set and consequently the cost/accuracy of the calculation are completely defined by (i) the B-spline parameters k, $R^0_{\rm max}$, $R^i_{\rm max}$ and $N_{\rm b}$, and (ii) the maximum value of the angular expansion $L^0_{\rm max}$ for the OCE and $L^i_{\rm max}$ for each set of non-equivalent centers.

Since the off-center radius spheres cannot intersect, the resulting Hamiltonian matrix $\mathbf{H}$ is partitioned into submatrices which are the diagonal elements $\mathbf{H}_{jj}$ and the blocks $\mathbf{H}_{0j}$ and $\mathbf{H}_{j0}$ between the set $\{\xi^0_{\alpha l_\alpha}\}$ and $\{\xi^i_{\alpha l_\alpha}\}$. The calculation of the non-diagonal block elements $\mathbf{H}_{0j}$ and $\mathbf{H}_{j0}$ represents the main computational effort because of the lack of analytical resolution. To carry out the integration, a numerical three-dimensional Gauss–Legendre scheme is employed. Also, a rotation of the coordinate framework of the main center of the spherical harmonics along the polar axis attached to the subsystems defined by the expansion centers leads to significant improvement. This exploits local cylindrical symmetry reducing integration to two variables (r and φ).

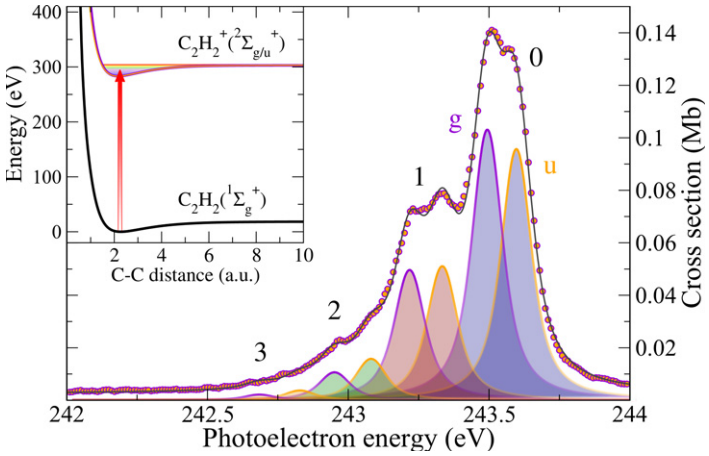

Figure 1. Photoelectron spectra of C_2H_2 taken at $h\upsilon = 534$ eV. Circles experimental results. Full lines: fit of the experimental data. Peak numbers indicate the vibrational quantum number v' of $C_2H_2^+$. The spectrum has been normalized to the value predicted by theory for the $^2\Sigma_u^+(1s\sigma_u, v' = 0)$ peak. Inset: potential energy curves of the ground state of C_2H_2 ($^1\Sigma_g^+$) (black line) and the $^2\Sigma_g^+(1s\sigma_g)$ (purple line) and $^2\Sigma_u^+(1s\sigma_u)$ (orange line) states of core-ionized $C_2H_2^+$ along the C–C symmetric-stretching normal coordinate. The red arrow indicates a vertical one-photon transition. The horizontal line in the upper potential energy curves indicates the dissociation limit and the shaded area below it the vibrational states in the $^2\Sigma_g^+(1s\sigma_g)$ and $^2\Sigma_u^+(1s\sigma_u)$ states.

The bound states are extracted by a generalized diagonalization of $\hat{H}_{KS}$ and continuum states by block inverse iteration [57] for each given photoelectron energy. Electronic dipole matrix elements were computed for 200 photoelectron energies, in a basis of 400 B-splines, a box size of 40 au and a maximum L value of 20.

The vibrational wave functions result from the solution of the vibrational Schrödinger equation in a basis of B-splines by using the projection of the potential energy surface along the C–C symmetric stretching coordinate. We have evaluated the vibrational wave functions by diagonalizing the vibrational Hamiltonian corresponding to this mode in a basis of 1000 B-splines within a box of 10 au. A similar method has been shown to provide accurate vibrationally resolved photoionization cross sections for N_2 and CO [14], as well as for CH_4 [42].

It is important to stress here that the present description of the C–C symmetric stretching vibrational mode is rather rudimentary, because in assuming that the C–H distance remains fixed during the vibration for both the parent molecule and the remaining ion, we neglect among other things the possible mixing between the two symmetric stretching modes associated with the electronic excitation (the Dushinsky effect) [58].

4. Results and discussion

Figure 1 shows the photoelectron spectrum at a photon energy of 534 eV. As can be seen, C 1s photoionization mainly leads to $C_2H_2^+$ ions in the ground vibrational state $v = 0$ of the C–C symmetric stretching mode. This is because the equilibrium geometries of C_2H_2 and $C_2H_2^+$ are very similar for this core-ionized electronic state. In other words, a vertical one-photon transition

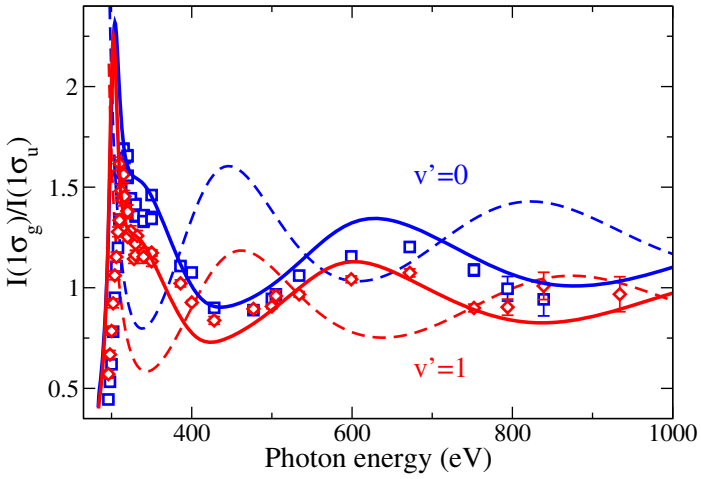

Figure 2. Vibrationally resolved $1\sigma_g/1\sigma_u$ ratios in C 1s photoionization of C_2H_2 for the C–C symmetric stretching mode of $C_2H_2^+$. Squares and diamonds: experimental results. The error bars include both statistical and systematic contributions. Full lines: theoretical results. Dashed lines: results from the simple model discussed in the text. No scaling has been applied to the calculated curves.

from the ground state of C_2H_2 necessarily leads to core ionized $C_2H_2^+$ with a geometry close to that of the ground state, so that the maximum Franck–Condon overlap corresponds to the $v = 0 \rightarrow v' = 0$ transition. For the same reason, the intensity of the observed peaks decreases rapidly with the degree of vibrational excitation of the remaining $C_2H_2^+$ ion and, for all practical purposes, it is negligible beyond $v' = 3$. Each v' peak is formed by two components, which correspond to C 1s ionization from the $1\sigma_g$ and $1\sigma_u$ molecular orbitals. The energy separation between these two components is 102.7 meV, in good agreement with the value of the $1\sigma_g$–$1\sigma_u$ splitting reported in previous work. As can be inferred from figure 1, the high energy resolution of the spectra allows us to clearly separate the two components.

The intensity in the photoelectron spectrum decreases very rapidly with photon energy. This rapid decrease, which also occurs in atoms, complicates the identification of interference effects. As reported in previous works [12, 14], a very elegant way of removing this rapid decrease from the analysis is to consider ratios of vibrational intensities (v-ratios), in which such a behavior is no longer present because both the numerator and the denominator decrease with a similar rate. An alternative way of removing this rapid decrease is to analyze the variation of the $1\sigma_g/1\sigma_u$ ratio with photon energy (see [16]).

Figures 2 and 3 show the measured and calculated $1\sigma_g/1\sigma_u$ and $v = 1/v = 0$ ratios as functions of photon energy. As can be seen, both ratios exhibit pronounced oscillations superimposed on a slowly increasing background. The agreement between theory and experiment is excellent. In particular, the theory reproduces quite well the differences between $1\sigma_g/1\sigma_u$ ratios associated with different vibrational states of the remaining $C_2H_2^+$ ion, as well as the phase opposition of the v-ratios in the $1\sigma_g$ and $1\sigma_u$ channels. Similar oscillations have been observed in $1\sigma_g/1\sigma_u$ ratios resulting from N 1s photoionization of N_2 [16]. In that work, the oscillations in the $1\sigma_g/1\sigma_u$ ratios have been interpreted as resulting from Cohen–Fano interferences. These interferences reflect a different phase in the $1\sigma_g$ and $1\sigma_u$ channels due to the difference in sign of the corresponding linear combinations of 1s orbitals.

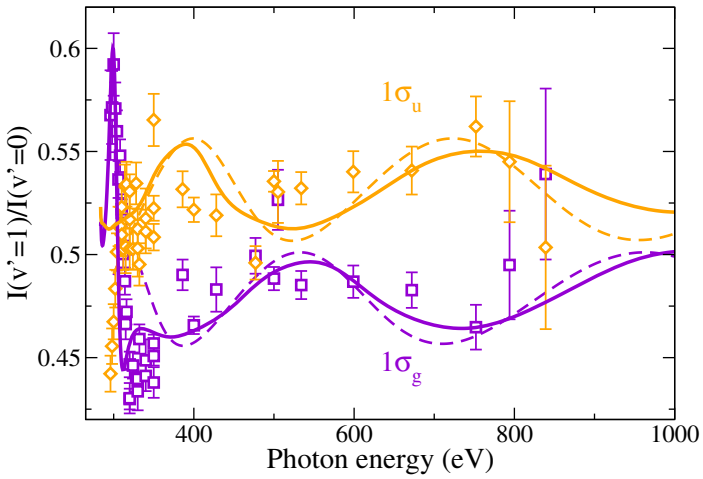

Figure 3. $v' = 1/v' = 0$ ratios between vibrationally resolved photoionization cross sections in C 1s photoionization of C_2H_2 for the C–C symmetric stretching mode of $C_2H_2^+$ in the σ_g and σ_u channels. Squares and diamonds: experimental results. The error bars include both statistical and systematic contributions. Full lines: theoretical results. Dashed lines: results from the simple model discussed in the text. The calculated curves have been rescaled so as to reproduce the experimental Franck-Condon ratio. See text for more details.

The similarity of the present $1\sigma_g/1\sigma_u$ ratios to those found in N 1s photoionization of N_2 suggests that the origin of the oscillations is the same. In order to ascertain that the observed features are indeed to be interpreted as genuine Cohen–Fano oscillations, we have developed a simple model in which, in addition to two-center interference effects, we also account for intramolecular scattering. As shown in [42] for C 1s photoionization of CH_4, the latter effect can lead to diffraction of the ejected electron and therefore to visible structures in the vibrationally resolved cross-section ratios.

In the model, the integral vibrationally resolved photoionization cross section $\sigma_\upsilon^{g/u}$ for a randomly oriented acetylene molecule is estimated within the single-active-electron approximation as (atomic units, au, are used hereafter unless otherwise specified)

$$\sigma_\upsilon^{g/u} = \frac{1}{4\pi}\int \mathrm{d}\Omega_R \int \mathrm{d}\Omega_k \quad 2\,\frac{4\pi^2 k}{c\omega}\,\left|\langle\,\psi_{\vec{k}}\,\chi_\upsilon^{g/u}|\,\hat{\epsilon}\cdot\vec{p}\,|\sigma_{g/u}\,\chi_0\rangle\right|^2. \tag{8}$$

Here χ_0 is the wave function of the ground vibrational state of the neutral molecule and $\chi_\upsilon^{g/u}$ is the vibrational wave function for the ionized state (either g or u) in either the $\upsilon = 0$ or $\upsilon = 1$ state of the C–C stretching vibrational mode. The initial core molecular orbital is approximated with a symmetry-adapted combination of the 1s core orbitals of the two carbon atoms as shown in equation (4). In momentum coordinates, this expression can be reformulated as

$$\sigma_{g/u}(\vec{p}) = \mathrm{e}^{-\mathrm{i}\vec{p}\cdot\vec{R}_{\mathrm{CC}}}\,\frac{\mathrm{e}^{\mathrm{i}\vec{p}\cdot\vec{R}/2} \pm \mathrm{e}^{-\mathrm{i}\vec{p}\cdot\vec{R}/2}}{\sqrt{2(1\pm S(R))}}\;1\mathrm{s}(p), \tag{9}$$

where the 1s orbital is now centered on the origin; $\vec{R}_{\mathrm{CC}} = (\vec{R}_{\mathrm{C}_1} + \vec{R}_{\mathrm{C}_2})/2$ indicates the center of mass of the two carbons and $\vec{R} = \vec{R}_{\mathrm{C}_2} - \vec{R}_{\mathrm{C}_1}$ is their relative position. The overlap $S(R)$ turns

out to be very small and will be neglected. The final electronic state is approximated with a plane wave:

$$\langle \vec{r} \,|\psi_{\vec{k}}\rangle = (2\pi)^{-3/2} \exp(\mathrm{i}\vec{k}\cdot\vec{r}), \tag{10}$$

therefore the transition amplitude in (8) becomes

$$\mathcal{A}_{\upsilon}^{g/u} = \langle \psi_{\vec{k}}\, \chi_{\upsilon}^{g/u} | \,\hat{\epsilon}\cdot\vec{p}\,|\sigma_{g/u}\,\chi_0\rangle = \frac{\hat{\epsilon}\cdot\vec{k}}{\sqrt{2}}\, 1s(k)\, \langle \chi_{\upsilon}^{g/u} \,|\, \mathrm{e}^{\mathrm{i}\vec{k}\cdot\vec{R}/2} \pm \mathrm{e}^{-\mathrm{i}\vec{k}\cdot\vec{R}/2} \,|\, \chi_0\rangle. \tag{11}$$

(In the last expression we dropped the term $\exp[-\mathrm{i}\vec{p}\cdot\vec{R}_{\mathrm{CC}}]$, related to the conservation of the total momentum of the CC moiety.) Based on these and other additional assumptions, several authors have already commented on the effect of the vibrational motion on Cohen–Fano oscillations [43, 59, 60]. As we will see below, the present model leads to qualitatively similar results.

As in the first-principles calculations, we will consider only the C–C symmetric stretching vibrational mode in which the C–H distance is kept constant:

$$\vec{R}_{\mathrm{C}_1} = -\vec{R}/2, \quad \vec{R}_{\mathrm{C}_2} = \vec{R}/2, \tag{12}$$

$$\vec{R}_{\mathrm{H}_1} = -(R/2 + R_{\mathrm{CH}})\hat{R}, \quad \vec{R}_{\mathrm{H}_2} = (R/2 + R_{\mathrm{CH}})\hat{R}. \tag{13}$$

To evaluate the vibrational transition amplitude in (11), we assume the harmonic approximation and that the vibrational frequency in both final parent ions is the same as that in the initial neutral molecule. In this context, we can express the internuclear distance in terms of the dimensionless vibrational normal coordinate of the neutral molecule,

$$R = R_0 + (\mu\omega)^{-1/2}\, Q, \tag{14}$$

while the final vibrational state $\chi_{\upsilon}^{g/u}$ can be written as the translation by a quantity equal to the shift in the equilibrium position, $\Delta R_0^{g/u} = R_0^{g/u} - R_0$, of the vibrational function χ_υ of the neutral molecule

$$\chi_{\upsilon}^{g/u} = \mathrm{e}^{-\mathrm{i}\sqrt{\mu\omega}\,\Delta R_0^{g/u}\,\hat{P}}\ \chi_\upsilon = D\left(\sqrt{\frac{\mu\omega}{2}}\,\Delta R_0^{g/u}\right)\ \chi_\upsilon. \tag{15}$$

In the last expression, $\hat{P}$ is the dimensionless momentum of the harmonic oscillator canonically conjugated to Q, $[Q, P] = i$, while the displacement operator $D(\alpha)$ is the generator of vibrational coherent states (see, e.g., paragraphs 3.3–9 in [61])

$$D(\alpha) = \mathrm{e}^{\alpha\hat{a}^\dagger - \alpha^*\hat{a}}, \quad |\alpha\rangle = D(\alpha)|0\rangle = \sum_{\upsilon} |\upsilon\rangle\, \mathrm{e}^{-|\alpha|^2/2}\frac{\alpha^\upsilon}{\sqrt{\upsilon!}}, \tag{16}$$

$$D^\dagger(\alpha) = D(-\alpha), \quad D(\alpha)D(\beta) = D(\alpha+\beta)\,\mathrm{e}^{(\alpha\beta^* - \beta\alpha^*)/2}. \tag{17}$$

In a similar way, the action of any exponential operator whose argument is linear in the normal coordinate Q can also be expressed in terms of displacement operators:

$$\mathrm{e}^{\mathrm{i}KQ} = D\left(\mathrm{i}\,\frac{K}{\sqrt{2}}\right). \tag{18}$$

By applying the relations listed above, after some passages, we are led to the expression

$$\begin{aligned}\langle \chi_\upsilon^{g/u} | \mathrm{e}^{\mathrm{i}p\,R} | \chi_0 \rangle &= \mathrm{e}^{\mathrm{i}p\,\bar{R}_0^{g/u}} \left\langle \upsilon \left| -\sqrt{\frac{\mu\omega}{2}}\,\Delta R_0^{g/u} + \mathrm{i}\frac{p}{\sqrt{2\mu\omega}} \right\rangle \right. \\ &= \mathrm{e}^{-\frac{p^2}{4\mu\omega}}\,\mathrm{e}^{\mathrm{i}p\,\bar{R}_0^{g/u}}\,\mathrm{e}^{-\frac{\mu\omega}{4}(\Delta R_0^{g/u})^2} \\ &\quad \times \frac{1}{\sqrt{\upsilon!}} \left(-\sqrt{\frac{\mu\omega}{2}}\,\Delta R_0^{g/u} + \mathrm{i}\,\frac{p}{\sqrt{2\mu\omega}} \right)^{\upsilon}, \end{aligned} \tag{19}$$

where $\bar{R}_0^{g/u} = (R_0 + R_0^{g/u})/2$. For $p = 0$, we recover the familiar Franck–Condon amplitude:

$$\langle \chi_\upsilon^{g/u} | \chi_0 \rangle = \mathrm{e}^{-\frac{\mu\omega}{4}(\Delta R_0^{g/u})^2}\,\frac{1}{\sqrt{\upsilon!}} \left(-\sqrt{\frac{\mu\omega}{2}}\,\Delta R_0^{g/u} \right)^{\upsilon}. \tag{20}$$

For the vibrational mode under consideration, the factor $\mu\omega$ is very large: $\mu \simeq 6.5$ amu $\simeq$ 12 000 au, $\omega \simeq 270$ meV $\simeq 0.01$ au, hence $\mu\omega \simeq 120$. The momentum factor p can be assumed to be of the same order of magnitude as that of the final momentum k of the photoelectron. For photoelectron energies up to $\sim$600 eV, the factor $\exp(-p^2/4\mu\omega)$ is thus very close to 1, so we will ignore it altogether. To be consistent with this approximation, we also need to drop all those terms arising from the expansion of the last power in equation (19) which are not linear in $p/\sqrt{2\mu\omega}$. To conclude, as long as $k^2/4\mu\omega \ll 1$, the following approximate expression can be used:

$$\langle\, \chi_\upsilon^{g/u} \,|\, \mathrm{e}^{\mathrm{i}p\,R} \,|\, \chi_0 \,\rangle \simeq \langle \chi_\upsilon^{g/u} | \chi_0 \rangle\, \mathrm{e}^{\mathrm{i}p\,\bar{R}_0^{g/u}} \left(1 - \mathrm{i}\frac{\upsilon\, p}{\mu\omega\,\Delta R_0^{g/u}} \right). \tag{21}$$

In the latter linearized form, this expression is essentially equivalent to equation (18) in [43], where no assumptions on the form of the vibrational functions were made.

By using the relations (21) in (11) we finally obtain the expression of the differential photoionization amplitudes for an oriented molecule

$$\begin{aligned}\mathcal{A}_\upsilon^g &\simeq \frac{\hat{\epsilon}\cdot\vec{k}}{\sqrt{2}}\,1\mathrm{s}(k)\,\langle \chi_\upsilon^g | \chi_0 \rangle \left[2\cos(\vec{k}\cdot\vec{\bar{R}}_0^g/2) + \upsilon\,\frac{\vec{k}\cdot\hat{R}}{\mu\omega\Delta R_0^g}\,\sin(\vec{k}\cdot\vec{\bar{R}}_0^g/2) \right], \\ \mathcal{A}_\upsilon^u &\simeq \frac{\hat{\epsilon}\cdot\vec{k}}{\sqrt{2}}\,1\mathrm{s}(k)\,\langle \chi_\upsilon^u | \chi_0 \rangle \left[2\mathrm{i}\sin(\vec{k}\cdot\vec{\bar{R}}_0^u/2) - \mathrm{i}\upsilon\,\frac{\vec{k}\cdot\hat{R}}{\mu\omega\Delta R_0^u}\,\cos(\vec{k}\cdot\vec{\bar{R}}_0^u/2) \right]. \end{aligned}$$

We can recover the familiar Cohen–Fano model from the latter expressions by retaining only the first term within parentheses. Note that in the present treatment the internuclear distance that appears in the final formula is intermediate between that in the neutral and that in the parent ion. As the second term in parentheses shows, the model accounts for the sensitivity of the interference amplitudes to the nuclear motion. This effect, which at this level is not visible in the amplitude for the transition to the ground vibrational state, is a manifestation of the nuclear recoil. Indeed, the factor $\exp(\mathrm{i}\vec{k}\cdot\vec{R}_i)$ can be seen as a boost by a momentum $\vec{k}$ on nucleus i. Nuclear recoil is therefore one of the mechanisms which mirror double-slit interferences to non-Franck–Condon vibrational excitations and which thus permits us to monitor the latter by looking at the $\sigma_1^{g/u}/\sigma_0^{g/u}$ ratios.

After taking the square module and carrying out the angular integrations,

$$\sigma_\upsilon^{g/u} = \frac{1}{4\pi} \int \mathrm{d}\Omega_R \int \mathrm{d}\Omega_k\, 2\,\frac{4\pi^2 k}{c\omega}\,\left|\mathcal{A}_\upsilon^{g/u}\right|^2, \tag{22}$$

the cross sections in plane wave approximation are finally obtained:

$$\sigma_\upsilon^{g/u} = 2\,\frac{16\pi^3 k^3}{3c\omega}\,1s^2(k)|\langle\chi_1^{g/u}|\chi_0\rangle|^2 \times\left[1 \pm \frac{\sin k\bar{R}_0^{g/u}}{k\bar{R}_0^{g/u}} \mp \frac{\upsilon k}{\mu\omega\Delta R_0^{g/u}}\,\frac{\cos(k\bar{R}_0^{g/u})}{k\bar{R}_0^{g/u}} \pm \frac{\upsilon}{\mu\omega\,\bar{R}_0^{g/u}\Delta R_0^{g/u}}\,\frac{\sin(k\bar{R}_0^{g/u})}{k\bar{R}_0^{g/u}}\right] \tag{23}$$

In agreement with the previous approximations, in this last expression we dropped the terms quadratic in υ. The last term in parentheses amounts to a correction of the amplitude of the Cohen–Fano oscillations. This term has not been considered in previous models. By neglecting this term, we end up with an equation similar to equation (20) of Ueda *et al* [43]. Indeed, by borrowing part of their notation, one obtains an expression formally identical to equations (22) and (23) in [43],

$$\sigma_\upsilon^{g/u} = 2\,\frac{16\pi^3 k^3}{3c\omega}\,1s^2(k)|\langle\chi_1^{g/u}|\chi_0\rangle|^2\,\left[1 \pm \chi_\upsilon^{g,u}(k)\right], \tag{24}$$

$$\chi_\upsilon^{g/u}(k) = \frac{\sin(k\bar{R}_0^{g/u} + \psi_\upsilon^{g,u}(k))}{\cos\psi_\upsilon^{g/u}(k)k\bar{R}_0^{g/u}}, \quad \tan\psi_\upsilon^{g/u} = -\frac{\upsilon k}{\mu\omega\Delta\bar{R}_0^{g/u}}. \tag{25}$$

The recoil thus induces an energy-dependent phaseshift $\psi_\upsilon^{g/u}(k)$ in the Cohen–Fano oscillations. Within the harmonic approximation adopted here, this phase shift is known analytically. A comparison with equation (23) in [43] leads to the following correspondence with the parametrization chosen by Ueda *et al*:

$$\Delta R_\upsilon = -\frac{\upsilon}{\mu\omega\Delta\bar{R}_0^{g/u}}. \tag{26}$$

What is indicated in [43] as an effective displacement ΔR_υ of the carbon–carbon internuclear distance appears, within the harmonic approximation, to be related in a simple way to the parameters of the vibrational mode. On the basis of equation (14), we can in fact recognize in $1/\sqrt{\mu\omega}$ the characteristic length R_ω of the oscillator and write the formula

$$\frac{\Delta R_\upsilon}{R_\omega} = -\upsilon\frac{R_\omega}{\Delta\bar{R}_0^{g/u}}. \tag{27}$$

The internuclear distances in the neutral are $R_0 = 2.273$ au, $R_{CH} = 2.002$ au. Theoretical estimates of the C–C internuclear distance exist [37]: $R_0^g = 2.198$ au, $R_0^u = 2.185$ au. With these values, $\bar{R}_0^g = 2.236$ au, $\bar{R}_0^u = 2.230$ au, $\Delta R_0^g = -0.075$ au and $\Delta R_0^u = -0.088$ au. In figure 3, the dashed lines show the $\upsilon = 1/\upsilon = 0$ intensity ratios computed with the complete formula (23). As can be seen from the figure, the model reproduces quite nicely the experimental and theoretical results. In particular, the model accounts for the phase opposition of the oscillations in the gerade and ungerade cases. The oscillation periods are some 2–3% larger than the $\Delta k \sim 2\pi/R_0^{g/u}$ values which are expected on the basis of simple dimensional considerations. A closer inspection of these results shows that the two ratios oscillate around baselines that start at the corresponding Franck–Condon ratios and increase with the photoelectron energy. The latter is due to the momentum transferred to either nuclei as the photoelectron is ejected (recoil). Since the amplitudes for the photoelectron ejection from the two nuclei add coherently, the momentum transfer, and therefore the vibrational excitation, is affected by the same interference

features observed in the total cross section. The largest discrepancy between the plane-wave prediction and the experiment is in the position of the baselines, i.e. in the Franck–Condon ratios $|\langle\chi_1^{g/u}|\chi_0\rangle/\langle\chi_0^{g/u}|\chi_0\rangle|^2$. The latter, however, depend strongly on the precise value of the contractions $\Delta R_0^{g/u}$ of the C–C bond length. It is possible that the theoretical estimates for the equilibrium positions in the parent ions given in [37] are not accurate enough. In fact, small adjustments of the order of 10^{-2} Å to $R_0^{g/u}$ are sufficient to bring the theoretical curves on top of the experimental ones. A similar discrepancy between theory and experiment is observed also in the case of the first-principles DFT calculations.

In contrast to the good agreement found for the vibrational ratios, the σ_g/σ_u ratios computed in the plane wave approximation turn out to be almost in phase opposition with respect to the measurements. The prediction of the model is shown in figure 2. In the case of the excited final vibrational state $\upsilon = 1$, the nuclear recoil induces a phase shift in the σ_g/σ_u ratio that partly reduces the distance with the experimental points. This effect, however, is still too small to compensate for the error of the Cohen–Fano prediction. Moreover, at the present level of approximation, the recoil does not have any effect on the $\upsilon = 0$ cross section. A major cause of the observed discrepancy must therefore be sought in a different mechanism. The phase shift difference between the $\upsilon = 0$ and the $\upsilon = 1$ cases predicted by the recoil should presumably show up in the experiment as well. Unfortunately, the present experimental accuracy does not allow us to draw any conclusion in this sense.

We have extended the present model beyond the plane-wave approximation [62] by including the contributions of the carbon and hydrogen Coulomb potentials in the first Born approximation. The corresponding results barely differ from those shown in figures 2 and 3, thus lending further support to our interpretation of the observed oscillations as resulting from two-center Cohen–Fano interferences.

5. Summary and conclusions

We have shown that vibrationally resolved C 1s photoelectron spectra of acetylene obtained with third-generation synchrotron radiation exhibit Cohen–Fano interferences similar to those previously reported in diatomic molecules. The oscillations are unambiguously observed in both the υ and g/u ratios, for which no independent estimation for the rapidly decreasing cross section is required. The results obtained from first-principles calculations based on density functional theory are in excellent agreement with the experimental measurements. The predictions of experiment and theory are further supported by a simple model that basically follows the premises of the original Cohen–Fano model developed for H_2^+. Although no quantitative agreement with either the experiment or the first-principles calculations is found, the qualitative features of the oscillations are correctly described: the overall period of the oscillations, the fact that the $\upsilon = 1/\upsilon = 0$ ratios for the gerade and ungerade cases are in phase opposition and the fact that there is no discernible influence of the nearby hydrogen atoms. These results confirm the delocalized character of the core hole created in the primary photoionization event and demonstrate that intramolecular core-hole coherence can survive the decoherence introduced by the asymmetric nuclear degrees of freedom that are characteristic of polyatomic molecules.

The conclusions reported in this work as well as those reported in [42] for CH_4 suggest that vibrationally resolved photoelectron spectroscopy can be used to determine the structure of polyatomic molecules in different environments, e.g. adsorbed on surfaces [63]. In the

latter case, photoelectron diffraction imaging makes use of holographic principles to extract information on the coordination of carbon atoms to a Si(100) surface. In a similar way, Cohen–Fano oscillations could give information on the C–C internuclear distance.

Finally, the ultrafast migration of holes in the valence shell has attracted considerable interest in recent years (see, e.g., [64, 65] and references therein). It will certainly be worth extending the ultra-fast time-resolved investigation to the dynamics of coherently created core-holes, too.

Acknowledgments

We thank Mare Nostrum BSC, Cineca and CCC-UAM (Centro de Computación Científica, Universidad Autónoma de Madrid) for the allocation of computer time. This work was supported by the MICINN project numbers FIS2010-15127, ACI2008-0777 and CSD 2007-00010 (Spain), the ERA-Chemistry project number PIM2010EEC-00751, the European COST Action CM0702 and the Marie Curie ITN CORINF. The experiment at SPring-8 was carried out with the approval of JASRI and was supported in part by grants in-aid for scientic research provided by the Japan Society for Promotion of Science. We thank the staff at SPring-8 for their help during the experiment. At SOLEIL Synchrotron (France), the experiment was performed at the PLEIADES beamline during beamtime allotted under proposal number 20100163. We are grateful to E Robert for technical assistance and to the SOLEIL staff for stable operation of the equipment and storage ring during the experiments.

References

[1] Cohen H D and Fano U 1966 Interference in the photo-ionization of molecules *Phys. Rev.* **150** 30
[2] Samson J A R and Cairns R A 1965 Total absorption cross sections of H_2, N_2 and O_2 in the region 550–200 Å *J. Opt. Soc. Am.* **55** 1035
[3] Stolterfoht N *et al* 2001 Evidence for interference effects in electron emission from H_2 colliding with 60 MeV/u Kr^{34+} ions *Phys. Rev. Lett.* **87** 023201
[4] Misra D *et al* 2004 Interference effect in electron emission in heavy ion collisions with H_2 detected by comparison with the measured electron spectrum from atomic hydrogen *Phys. Rev. Lett.* **92** 153201
[5] Kamalou O *et al* 2005 Evidence for interference effects in both slow and fast electron emission from D_2 by energetic electron impact *Phys. Rev.* A **71** 010702
[6] Milne-Brownlie D *et al* 2006 Young-type interference in (e,2e) ionization of H_2 *Phys. Rev. Lett.* **96** 233201
[7] Akoury D *et al* 2007 The simplest double slit: interference and entanglement in double photoionization of H_2 *Science* **318** 949
[8] Kreidi K *et al* 2008 Interference in the collective electron momentum in double photoionization of H_2 *Phys. Rev. Lett.* **100** 133005
[9] Díez Muiño R *et al* 2002 Angular distributions of electrons photoemitted from core levels of oriented diatomic molecules: multiple scattering theory in non-spherical potentials *J. Phys. B: At. Mol. Opt. Phys.* **35** L359
[10] Fojón O *et al* 2004 Interference effects in H_2 photoionization at high energies *J. Phys. B: At. Mol. Opt. Phys.* **37** 3035
[11] Fernández J, Fojón O, Palacios A and Martín F 2007 Interferences from fast electron emission in molecular photoionization *Phys. Rev. Lett.* **98** 043005
[12] Fernández J, Fojón O and Martín F 2009 Double-slit, confinement and non-Franck–Condon effects in photoionization of H_2 at high photon energy *Phys. Rev.* A **79** 023420

[13] Fernández J *et al* 2009 Two-center effects in one-photon single ionization of H_2^+, H_2 and Li_2^+ with circularly polarized light *Phys. Rev.* A **79** 043409
[14] Canton S E *et al* 2011 Direct observation of Young's double-slit interferences in vibrationally resolved photoionization of diatomic molecules *Proc. Natl Acad. Sci. USA* **108** 18 7302
[15] Becker U 2011 Matter-wave interference made clear *Nature* **474** 586
[16] Semenov S K *et al* 2006 Interference modulation in the vibrationally resolved photoionization of the 1σ g and 1σ u core levels of the N_2 molecule *J. Phys. B: At. Mol. Opt. Phys.* **39** L261
[17] Rolles D *et al* 2005 Isotope-induced partial localization of core electrons in the homonuclear molecule N_2 *Nature* **437** 7059–711
[18] Schöffler M *et al* 2008 Ultrafast probing of core hole localization in N_2 *Science* **320** 920
[19] Ueda K 2010 Which-pass information in the double-slit experiment of diatomic molecules *J. Phys.: Conf. Series* **212** 012033
[20] Schöffler M *et al* 2011 Matter wave optics perspective at molecular photoionization: K-shell photoionization and Auger decay of N_2 *New J. Phys.* **13** 095013
[21] Hergenhahn U *et al* 2001 Symmetry-selective observation of the N 1s shape resonance in N_2 *J. Phys. Chem.* A **105** 5704
[22] Zimmermann B *et al* 2008 Localization and loss of coherence in molecular double-slit experiments *Nat. Phys.* **4** 649
[23] Adachi J, Kosugi N, Shigemasa E and Yagishita A 1995 Renner–Teller effect and Rydberg-valence mixing in the N and O K-edge photoabsorption spectra of N_2O *J. Chem. Phys.* **102** 7369
[24] Adachi J, Kosugi N, Shigemasa E and Yagishita A 1997 Renner–Teller splitting in the C $1s \rightarrow \pi^*$ excited states of CS_2, OCS and CO_2 *J. Chem. Phys.* **107** 4919
[25] Miron C *et al* 2001 Nuclear motion driven by the Renner–Teller effect as observed in the resonant Auger decay to the $\bar{X}\,^2\Pi$ electronic ground state of N_2O^+ *J. Chem. Phys.* **115** 864
[26] Kimberg V, Kosugi N and Gel'mukhanov F 2009 Theoretical studies of angle-resolved ion yield spectra of core-to-valence transitions of acetylene *J. Chem. Phys.* **130** 114302
[27] Miron C *et al* 2010 Vibrational scattering anisotropy generated by multichannel quantum interference *Phys. Rev. Lett.* **105** 093002
[28] Gadea F X *et al* 1991 Vibronic coupling and core-hole localization in K-shell excitations of ethene *Phys. Rev. Lett.* **66** 883
[29] Broer R and Nieuwpoort W C 1999 Hole localization and symmetry breaking *J. Mol. Struct.* **458** 19
[30] Snyder L C 1971 Core–electron binding energies and Slater atomic shielding constants *J. Chem. Phys.* **55** 95
[31] Domcke W and Cederbaum L S 1977 Vibronic coupling and symmetry breaking in core electron ionization *Chem. Phys.* **25** 189
[32] Kivimäki A *et al* 1997 Vibrationally resolved O 1s photoelectron spectrum of CO_2: vibronic coupling and dynamic core-hole localization *Phys. Rev. Lett.* **79** 998
[33] Gunnelin K *et al* 1999 Bond-length-dependent core hole localization observed in simple hydrocarbons *Phys. Rev. Lett.* **83** 1315
[34] Kempgens B *et al* 1997 Core level energy splitting in the C 1s photoelectron spectrum of C_2H_2 *Phys. Rev. Lett.* **79** 3617
[35] Karlsen T *et al* 2001 Vibrational structure and vibronic coupling in the carbon 1s photoelectron spectra of ethane and deuteroethane *J. Phys. Chem.* A **105** 7700
[36] Lievin J *et al* 2011 Comparison of the experimental, semi-experimental and *ab initio* equilibrium structures of acetylene: influence of relativistic effects and of the diagonal Born–Oppenheimer corrections *J. Chem. Phys.* **134** 064119
[37] Börve K *et al* 2000 Vibronic structure in the carbon 1s photoelectron spectra of HCCH and DCCD *Phys. Rev.* A **63** 012506
[38] Thomas T D *et al* 1999 Photon energy dependence of the $1\sigma_u/1\sigma_g$ intensity ratio in carbon 1s photoelectron spectroscopy of ethyne *Phys. Rev. Lett.* **82** 1120

[39] Hoshino M *et al* 2006 Symmetry- and vibrationally-resolved C K-shell photoionization studies of C_2H_2 *Chem. Phys. Lett.* **421** 256
[40] Adachi J-I *et al* 2007 Photoelectron–photoion–photoion momentum spectroscopy as a direct probe of the core-hole localization in C 1*s* photoionization of C_2H_2 *J. Phys. B: At. Mol. Opt. Phys.* **40** F285
[41] Osipov T *et al* 2008 Fragmentation pathways for selected electronic states of the acetylene dication *J. Phys. B: At. Mol. Opt. Phys.* **41** 091001
[42] Plésiat E *et al* 2012 *Phys. Rev.* A **85** 023409
[43] Ueda K *et al* 2006 Role of the recoil effect in two-center interference in x-ray photoionization *Chem. Phys.* **329** 329
[44] Ueda K 2003 High-resolution inner-shell spectroscopies of free atoms and molecules using soft-x-ray beamlines at the third-generation synchrotron radiation sources *J. Phys. B: At. Mol. Opt. Phys.* **36** R1
[45] Miron C *et al* 2009 PLEIADES: an ultra high resolution soft x-rays beamline for advanced spectroscopic studies on diluted species www.synchrotron-soleil.fr/Recherche/LignesLumiere/PLEIADES
[46] Travnikova O *et al* 2010 Circularly polarized x-rays: another probe of ultrafast molecular decay dynamics *Phys. Rev. Lett.* **105** 233001
[47] Söderström J *et al* 2011 Angle-resolved electron spectroscopy of the resonant Auger decay in xenon with meV energy resolution *New J. Phys.* **13** 073014
[48] Miron C *et al* 2011 Imaging molecular potentials using ultrahigh-resolution resonant photoemission *Nat. Phys.* **8** 135–8
[49] Sun Y-P, Wang C-K and Gel'mukhanov F 2010 Rotational doppler effect in x-ray photoionization *Phys. Rev.* A **82** 052506
[50] Thomas T D *et al* 2011 Experimental observation of rotational Doppler broadening in a molecular system *Phys. Rev. Lett.* **106** 193009
[51] Myrseth V *et al* 2002 Adiabatic and vertical carbon 1s ionization energies in representative small molecules *J. Electron Spectrosc. Relat. Phenom.* **122** 57
[52] Kukk E www.physics.utu.fi/en/research/material_SUBSCRIPTNBscience/Fitting.html
[53] van der Straten P, Morgenstern R and Niehaus A 1988 Angular dependent post-collision interaction in auger processes *Z. Phys.* D **8** 35
[54] Carroll T X *et al* 2002 Carbon 1s photoelectron spectroscopy of CF_4 and CO: search for chemical effects on the carbon 1s hole-state lifetime *J. Chem. Phys.* **116** 10221
[55] Bachau H *et al* 2001 Application of B-splines in atomic and molecular physics *Rep. Prog. Phys.* **64** 1815
[56] Fonseca Guerra C, Snijders J G, te Velde G and Baerends E J 1998 Towards an order-*N* DFT method *Theor. Chem. Acc.* **99** 391
[57] Venuti M, Stener M and Decleva P 1998 Valence photoionization of C_6H_6 by the B-spline one-centre expansion density functional method *Chem. Phys.* **234** 95
[58] Duschinsky F 1937 On the interpretation of electronic spectra of polyatomic molecules *Acta Physicochim. URSS* **7** 551
[59] Domcke W and Cederbaum L S 1978 Electronic recoil effects in high-energy photoelectron spectroscopy *J. Electron Spectrosc. Relat. Phenom.* **13** 161
[60] Gel'mukhanov F *et al* 2007 Young's double-slit experiment using two-center core-level photoemission: photoelectron recoil effects *J. Electron Spectrosc. Relat. Phenom.* **158** 265
[61] Vourdas A 2006 Analytic representations in quantum mechanics *J. Phys. A: Math. Gen.* **39** R65
[62] Argenti L, Plésiat E, Decleva P and Martín F in preparation
[63] Xu S *et al* 2000 Photoelectron diffraction imaging for C_2H_2 and C_2H_4 chemisorbed on Si(100) reveals a new bonding configuration *Phys. Rev. Lett.* **84** 939
[64] Lünnemann S, Kuleff A I and Cederbaum L S 2009 Ultrafast electron dynamics following outer-valence ionization: the impact of low-lying relaxation satellite states *J. Chem. Phys.* **130** 154305
[65] Kuleff A I and Cederbaum L S 2011 Radiation generated by the ultrafast migration of a positive charge following the ionization of a molecular system *Phys. Rev. Lett.* **106** 053001